THE INTERNATIONAL JOURNAL OF SCIENCE & TECHNOLEDGE

Influence of Chemical Reaction, Magnetic Field, Heat Source on Heat and Mass Transfer by Free Convection Flow over a Stretching Cone Embedded in a Porous Medium Considering Soret and Dufour Effects

Bishwa Ram Sharma
Professor, Department of Mathematics, Dibrugarh, Assam, India
Animesh Aich
Research Scholar, Department of Mathematics, Dibrugarh, Assam, India

Abstract:
Heat and mass transfer characteristics of free convection flow over a stretching cone embedded in a porous medium subjected to a chemical reaction, magnetic field, heat source are investigated numerically by taking into account the Soret and Dufour effects. The velocity, temperature and concentration profiles are drawn for various values of heat source parameter, pressure work parameter, magnetic field parameter, Rayleigh number, chemical reaction parameter, buoyancy ratio parameter, Prandtl number, Schmidt number, thermal stratification parameter, wall concentration exponent, Soret and Dufour numbers. Numerical results of rate of heat and mass transfer for different parameters are presented in tabular form and the results are depicted graphically.

Keywords: *Heat and mass transfer, chemical reaction, magnetic field, heat source, thermal stratification, wall concentration exponent, Soret and Dufour effects*

1. Introduction

Convective flow through porous media has attracted considerable attention in last several decades due to its many important engineering, environmental and geophysical applications. The combined heat and mass transfer problems with chemical reactions are investigated by many researchers in recent years. Andersson [1] studied the diffusion of a chemically-reactive species from a stretching sheet. Anjali Devi and Kandasamy [2] have analyzed the effects of chemical reaction, heat and mass transfer on laminar flow with along a semi infinite horizontal plate. Muthucumaraswamy and Ganeshan [3] studied the effects of suction on heat and mass transfer along a moving vertical surface in the presence of chemical reaction. Hering and Grosh [4] discussed the laminar natural convection from a non-isothermal cone at low Prandtl numbers. Roy [5] studied the free convection from a vertical cone at high Prandtl numbers.. Yih [6] investigated the effect of uniform lateral mass flux on free convection about a vertical cone embedded in a fluid-saturated porous medium. Hossain [7] discussed non-Darcy natural convection heat and mass transfer along a vertical permeable cylinder embedded in a porous medium. Chamkha [8] studied simultaneous heat and mass transfer by natural convection about a vertical wedge and a cone embedded in a porous medium. Mahdy and Mohamed [9] discussed the influence of magnetic field on natural convection flow near a wavy cone in porous media. Muthucumaraswamy [10] analysed the effects of a chemical reaction on a moving isothermal vertical infinitely long surface with suction. Anjali Devi and Kandasamy [11] studied the effects of chemical reaction, heat and mass transfer on non-linear MHD laminar boundary layer flow over a wedge with suction and injection. Joshi and Gebhart [12] investigated the effect of pressure stress work and viscous dissipation in some natural convection flows. Chamkha and Mansour [13] analysed the effects of chemical reaction and pressure work on free convection over a stretching cone embedded in a porous medium. Postelnicu [14] studied the influence of chemical reaction on heat and mass transfer by natural convection from vertical surfaces in porous media considering Soret and Dufour effects. Cheng [15] investigated the Soret and Dufour effects on natural convection heat and mass transfer from a vertical cone in porous media. Awad and Sibanda [16] studied the heat and mass transfer from an inverted cone in a porous medium with cross-diffusion effects. Chamkha and Rashad [17] analysed the Heat and Mass transfer by natural convection flow about a truncated cone in porous media with Soret and Dufour effects.

The objective of this paper is to study the effect of chemical reaction, heat source, thermal-diffusion and diffusion-thermal effects on MHD heat and mass transfer free convection flow over a stretching cone embedded in a porous medium.

2. Mathematical Formulation

We consider steady, laminar, two dimensional MHD free convective flow together with heat and mass transfer of a viscous incompressible electrically conducting fluid along a stretched cone of radius $'r'$ embedded in a porous medium. The effects of

thermal-diffusion, diffusion-thermal, heat source, a first order homogenous chemical reaction and uniform magnetic field on flow, heat and mass transfer are taken into account. The fluid properties are assumed to be constant except the density terms in the buoyancy terms of the momentum equations. The surface of the cone is maintained at a constant temperature T_w and a constant concentration C_w .The ambient temperature and concentration far away from the surface of the cone which is assumed to be uniform is T_∞ and C_∞ where $T_w > T_\infty$ and $C_w > C_\infty$. The physical model and coordinate system is as shown in the figure 1.

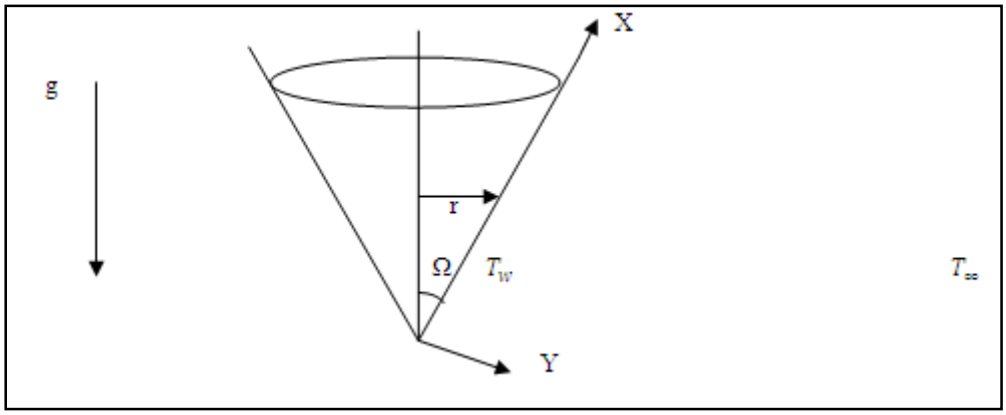

Figure 1: Physical model and coordinate system

Under the Boussinesq approximation, the governing equations are given by

$$\frac{\partial(ru)}{\partial x} + \frac{\partial(rv)}{\partial y} = 0 , \quad \ldots(1)$$

$$u\left(1 + \frac{k_1\sigma\mu_e^2H_0^2}{\mu}\right)\frac{\partial u}{\partial y} = \frac{k_1 g\cos(\Omega)}{\nu}\left(\beta_T\frac{\partial T}{\partial x} + \beta_C\frac{\partial C}{\partial y}\right), \quad \ldots(2)$$

$$u\frac{\partial T}{\partial x} + v\frac{\partial T}{\partial y} = \frac{k}{\rho C_P}\frac{\partial^2 T}{\partial y^2} + \frac{\beta_T T_f}{\rho C_P}u\frac{dP}{dx} + \frac{Q_0}{\rho C_P}(T - T_\infty) + \frac{Dk_T}{C_s C_P}\frac{\partial^2 C}{\partial y^2} \quad \ldots(3)$$

$$u\frac{\partial C}{\partial x} + v\frac{\partial C}{\partial y} = D\frac{\partial^2 C}{\partial y^2} + \frac{Dk_T}{T_m}\frac{\partial^2 T}{\partial y^2} - k_c(C - C_\infty) \quad \ldots(4)$$

where u and v are the velocity components in x and y directions respectively, g is the acceleration due to gravity, C and T denote the concentration and temperature of the fluid, ρ is the density, β_T is the coefficient of thermal expansion, β_C is coefficient of concentration expansion, σ is the fluid electrical conductivity, H_o is the strength of applied magnetic field, μ_e is the magnetic permeability, k_1 is the permeability of porous medium, μ and ν are dynamic and kinematic viscosities, k and C_P are the thermal conductuvity and specific heat of the fluid, ρ is the density of the fluid, Q_0 is heat generation or absorption constant, D is mass diffusitivity, k_T is thermal diffusion ratio, C_s is concentration susceptibility, T_f is the film temperature, T_m is the mean fluid temperature and k_c is the rate of chemical reaction.

The fluid pressure according to [12] is given by $\frac{dP}{dx} = -\rho g$ ...(5)

The initial and boundary conditions of the problem are

$$\left.\begin{array}{l} v = 0, T = T_w , C = C_w \text{ at } y = 0 \\ u \to 0, T \to T_\infty , C \to C_\infty \text{ as } y \to \infty \end{array}\right\} \quad \ldots(6)$$

The similarity transformations are given by

$$\left.\begin{array}{l} \Psi = r(x)\left(\nu x U(x)\right)^{\frac{1}{2}} f(\eta), \ \eta = \left(\frac{U(x)}{\nu x}\right)^{\frac{1}{2}} y \\ \theta(\eta, x) = \frac{T - T_\infty}{T_w - T_\infty} , \emptyset(\eta, x) = \frac{C - C_\infty}{C_w - C_\infty} , \ T_w - T_\infty = sx^n , C_w - C_\infty = s_1 x^{n_1}, U(x) = ax \end{array}\right\} \quad \ldots(7)$$

where n is a constant called the thermal stratification constant, n_1 is a constant called the wall concentration exponent, a, s and s_1 are all constant.

The modified stream function is introduced by the equations

$$ru = \frac{\partial\psi}{\partial y} , \ rv = -\frac{\partial\psi}{\partial x} \quad \ldots(8)$$

If we introduce the relations (7) into the equations (2), (3)and(4), then we have

$$(1 + M^2)f''' - Ra(\theta' + N\emptyset') = 0 , \quad \ldots(9)$$

$$\theta'' + \Pr(2f\theta' - nf'\theta + Q\theta - \varepsilon f' + D_f\phi'') = 0 \quad \ldots(10)$$

and

$$\phi'' + S_c(2f\emptyset' - \gamma\emptyset - n_1 f'\emptyset + Sr\theta'') = 0 \quad \ldots(11)$$

where $M = \frac{k_1\sigma\mu_e^2H_0^2}{\mu}$ is the magnetic field parameter, $Ra = \frac{k_1 g\beta_T(T_w - T_\infty)\cos(\Omega)}{\nu U}$ is the Rayleigh number, $N = \frac{\beta_C(C_w - C_\infty)}{\beta_T(T_w - T_\infty)}$ is the buoyancy ratio parameter, $Pr = \frac{\mu C_P}{k}$ is the Prandtl number, $Q = \frac{Q_0}{a\rho C_P}$ is the heat generation or absorption parameter, $\varepsilon = \frac{\beta_T T_f g U}{aC_P(T_w - T_\infty)}$ is the

pressure work parameter, $D_f = \frac{Dk_T(C_w - c_\infty)}{C_s C_P \nu(T_w - T_\infty)}$ is the Dufour number, $Sc = \frac{\nu}{D}$ is the Schmidt number, $S_r = \frac{Dk_T(T_w - T_\infty)}{T_m \nu(C_w - C_\infty)}$ is the Soret number and $\gamma = \frac{k_c}{a}$ is chemical reaction parameter.

The initial and boundary conditions (7) becomes

$$\left.\begin{array}{ll} f = 0,\ \theta = 1, \emptyset = 1 & \text{at } \eta = 0 \\ f' \to 0, \theta \to 0, \emptyset \to 0 & \text{at } \eta \to \infty \end{array}\right\} \quad \ldots(12)$$

3. Results and Discussions

The ordinary differential equations (9) , (10) and (11) with the corresponding boundary conditions (12) have been solved numerically by using bvp4c solver of MATLAB. From the process of numerical computation , the local Nusselt number and the local Sherwood number which are proportional to $-\theta'(0)$ and $-\emptyset'(0)$ respectively are worked out and their numerical values are presented in tabular form. Numerical calculations for $\theta'$and $\emptyset'$ have been carried out by taking various values of parameters $M, Ra, N, Pr, \varepsilon, Q, D_f, n, Sc, \gamma, S_r,$ and n_1. Several cases are considered:

CaseI:- $Ra = 1, N = 1, Pr = 0.71, \varepsilon = 1, Q = 0.5, D_f = 0.5, n = 0.5, Sc = 0.62, \gamma = 1, S_r = 0.5, n_1 = 0.5, M = (1,2,3)$

CaseII:- $M = 1, N = 1, Pr = 0.71, \varepsilon = 1, Q = 0.5, D_f = 0.5, n = 0.5, Sc = 0.62, \gamma = 1, S_r = 0.5, n_1 = 0.5, Ra = (0.5,1.0,1.5)$

CaseIII:- $M = 1, Ra = 1, Pr = 0.71, \varepsilon = 1, Q = 0.5, D_f = 0.5, n = 0.5, Sc = 0.62, \gamma = 1, S_r = 0.5, n_1 = 0.5, N = (0.5,1.0,1.5)$

CaseIV:-$M = 1, Ra = 1, N = 1, \varepsilon = 1, Q = 0.5, D_f = 0.5, n = 0.5, Sc = 0.62, \gamma = 1, S_r = 0.5, n_1 = 0.5, Pr = (0.71,1.0,2.0)$

CaseV:- $M = 1, Ra = 1, N = 1, Pr = 0.71, Q = 0.5, D_f = 0.5, n = 0.5, Sc = 0.62, \gamma = 1, S_r = 0.5, n_1 = 0.5, \varepsilon = (0.5,1.0,1.5)$

CaseVI:- $M = 1, Ra = 1, N = 1, Pr = 0.71, \varepsilon = 1, D_f = 0.5, n = 0.5, Sc = 0.62, \gamma = 1, S_r = 0.5, n_1 = 0.5, Q = (0.0,0.5,1.0)$

CaseVII:- $M = 1, Ra = 1, N = 1, Pr = 0.71, \varepsilon = 1, Q = 0.5, n = 0.5, Sc = 0.62, \gamma = 1, S_r = 0.5, n_1 = 0.5, D_f = (0.5,1.0,1.5)$

CaseVIII:- $M = 1, Ra = 1, N = 1, Pr = 0.71, \varepsilon = 1, Q = 0.5, D_f = 0.5, Sc = 0.62, \gamma = 1, S_r = 0.5, n_1 = 0.5, n = (0.2,0.5,0.8)$

CaseIX:- $M = 1, Ra = 1, N = 1, Pr = 0.71, \varepsilon = 1, Q = 0.5, D_f = 0.5, n = 0.5, \gamma = 1, S_r = 0.5, n_1 = 0.5, Sc = (0.35,0.62,1.0)$

CaseX:- $M = 1, Ra = 1, N = 1, Pr = 0.71, \varepsilon = 1, Q = 0.5, D_f = 0.5, n = 0.5, Sc = 0.62, S_r = 0.5, n_1 = 0.5, \gamma = (1,2,3)$

CaseXI:- $M = 1, Ra = 1, N = 1, Pr = 0.71, \varepsilon = 1, Q = 0.5, D_f = 0.5, n = 0.5, Sc = 0.62, , \gamma = 1, n_1 = 0.5, S_r = (0.5,1.0,1.5)$

CaseXII:- $M = 1, Ra = 1, N = 1, Pr = 0.71, \varepsilon = 1, Q = 0.5, D_f = 0.5, n = 0.5, Sc = 0.62, , \gamma = 1, S_r = (0.5), n_1 = (0.2,0.5,0.8)$

3.1. Case I:

Figures 2(a)-(c) exhibit velocity, temperature and concentration profile for various values of magnetic field parameter M . It is observed that the velocity, temperature and concentration decrease exponentially from their maximum values at the surface to their minimum values at the end of the boundary layer. Figure 2(a) exhibits that with the increase in the values of M, velocity of the fluid decreases in the boundary layer region $0 < \eta < 1.5$ and reverse effect is noticed in the boundary layer region $1.5 < \eta < 4.4$. The velocity of the fluid becomes minimum in the region $\eta > 4.4$ for all the values of M. Figure 2(b) exhibits that with the increase in the value of M, temperature of the fluid increases in the boundary layer region $0 < \eta < 6$ and no effect is observed from $\eta = 6$ onwards. Figure 2(c) exhibits that with the increase in the value of M, concentration of the fluid increases slightly in the boundary layer region $0 < \eta < 4.2$ and it becomes minimum in the region $\eta > 4.2$ for all the values of M.

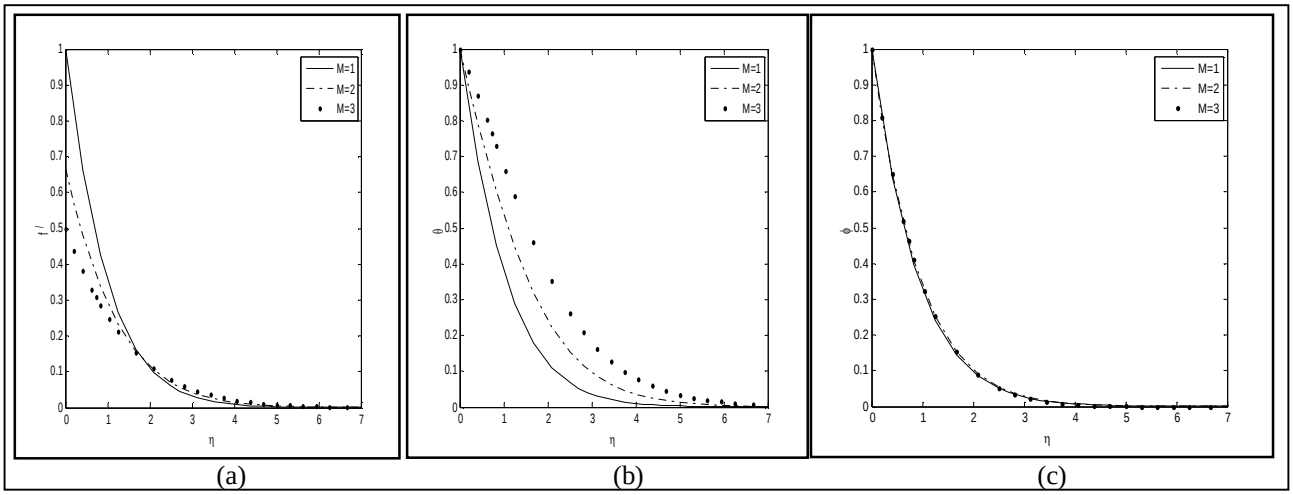

Figure 2: Effect of Magnetic field parameter M on (a) the velocity profiles, (b) the temperature profiles, (c) the concentration profiles

3.2. Case II:

Figures 3(a)-(c) exhibit velocity, temperature and concentration profile for various values of Rayleigh number Ra . It is observed that the velocity, temperature and concentration decrease exponentially from their maximum values at the surface to their minimum values at the end of the boundary layer. Figure 3(a) exhibits that with the increase in the values of Ra, velocity of the fluid increases in the boundary layer region $0 < \eta < 1.5$ and reverse effect is noticed in the boundary layer region $1.5 < \eta < 5$. The velocity of the fluid

becomes minimum in the region $\eta > 5$ for all the values of Ra. Figure 3(b) exhibits that with the increase in the value of Ra, temperature of the fluid decreases throughout in the boundary layer region $0 < \eta < 7$. Figure 3(c) exhibits that with the increase in the value of Ra, concentration of the fluid decreases slightly in the boundary layer region $0 < \eta < 4$ and it becomes minimum in the region $\eta > 4$ for all the values of Ra.

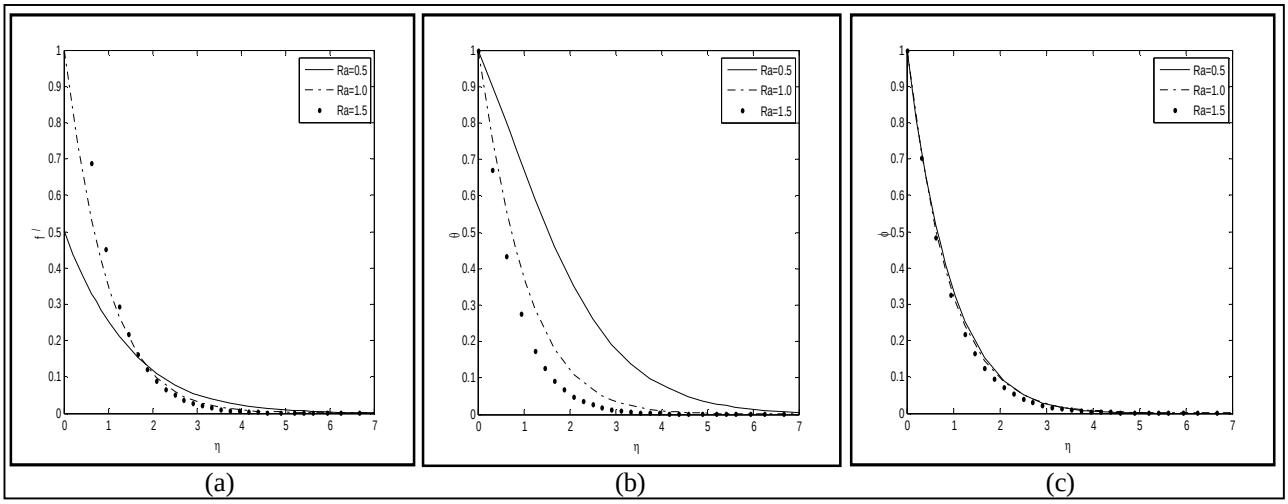

(a) (b) (c)

Figure 3: Effect of Rayleigh number Ra on (a) the velocity profiles, (b) the temperature profiles, (c) the concentration profiles.

3.3. Case III:

Figures 4(a)-(c) exhibits temperature and concentration profile for various values of buoyancy ratio parameter N. It is observed that the velocity, temperature and concentration decrease exponentially from their maximum values at the surface to their minimum values at the end of the boundary layer. Figure 4(a) exhibits that with the increase in the values of N, velocity of the fluid increases in the boundary layer region $0 < \eta < 1.5$ and reverse effect is noticed in the boundary layer region $1.5 < \eta < 4.4$. The velocity of the fluid becomes minimum in the region $\eta > 4.4$ for all the values of N. Figure 4(b) exhibits that with the increase in the value of N, temperature of the fluid decreases in the boundary layer region $0 < \eta < 5$ and no effect is observed from $\eta = 5$ onwards. Figure 4(c) exhibits that with the increase in the value of N, concentration of the fluid decreases slightly in the boundary layer region $0 < \eta < 4.2$ and it becomes minimum in the region $\eta > 4.2$ for all the values of N.

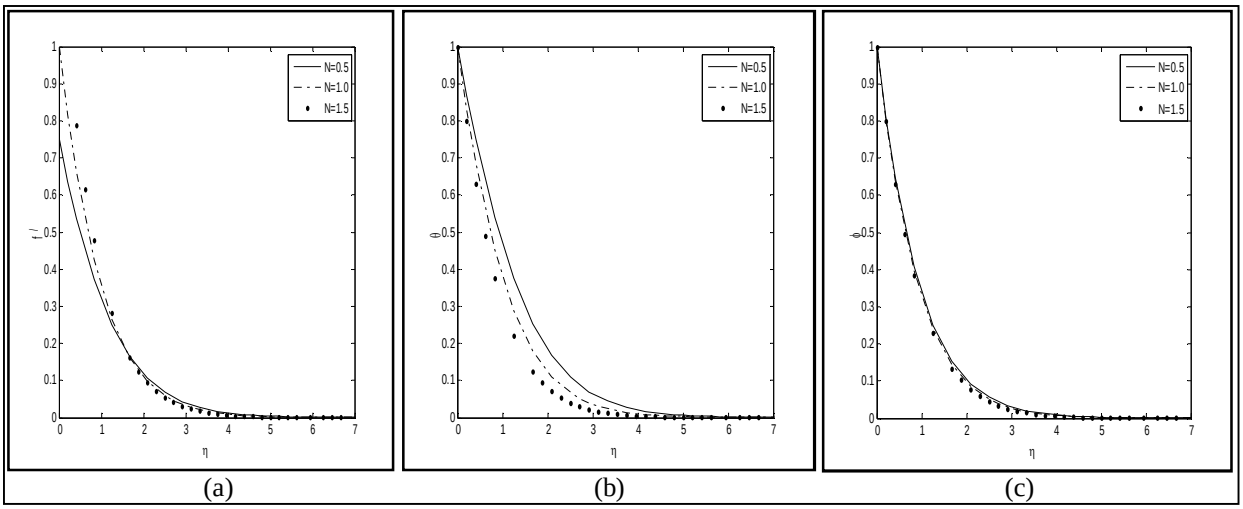

(a) (b) (c)

Figure 4: Effect of buoyancy ratio parameter N on (a) the velocity profiles, (b) the temperature profiles, (c) the concentration profiles

3.4. Case IV:

Figures 5(a)-(c) exhibits velocity,temperature and concentration profile for various values of prandtl number Pr. It is observed that the velocity, temperature and concentration decrease exponentially from their maximum values at the surface to their minimum values at the end of the boundary layer. Figure 5(a) exhibits that with the increase in the values of Pr, velocity of the fluid decreases in $0 < \eta < 1.5$ and reverse effect is noticed in the boundary layer region $1.5 < \eta < 7$. Figure 5(b) exhibits that with the increase in the value of Pr, temperature of the fluid decreases in the boundary layer region $0 < \eta < 5$ and it becomes minimum in the region $\eta > 5$ for all the values of Pr. Figure 5(c) exhibits that with the increase in the value of Pr, concentration of the fluid increases in the boundary layer region $0 < \eta < 7$.

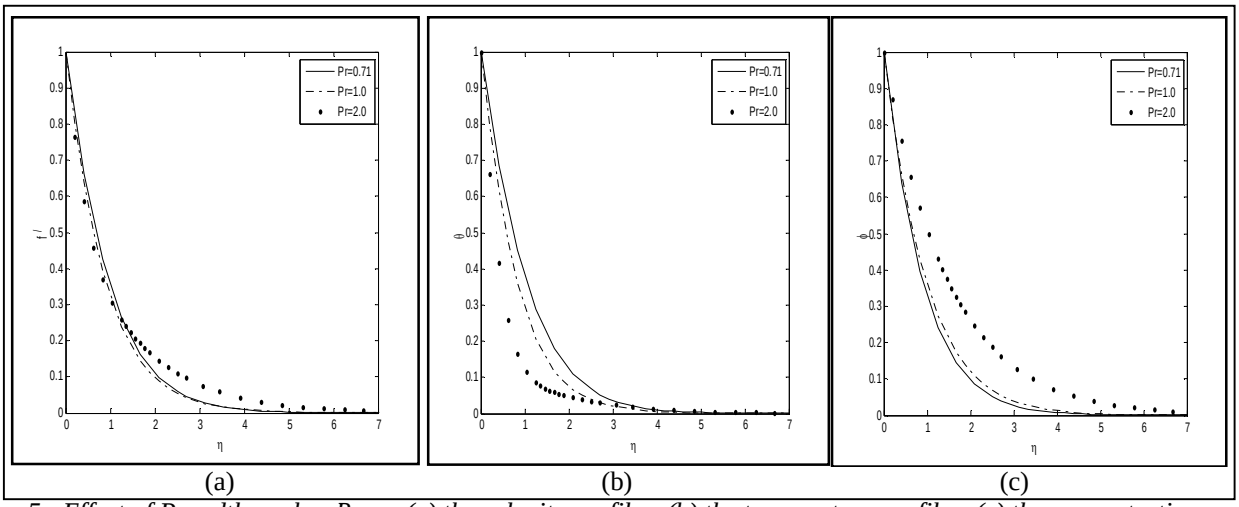

Figure 5 : Effect of Prandtl number Pr on (a) the velocity profiles, (b) the temperature profiles, (c) the concentration profiles

3.5. Case V:

Figures 6(a)-(c) exhibits velocity, temperature and concentration profile for various values of pressure work parameter ϵ It is observed that the velocity, temperature and concentration decrease exponentially from their maximum values at the surface to their minimum values at the end of the boundary layer. Figure 6(a) exhibits that with the increase in the values of parameter ϵ, velocity of the fluid decreases in the boundary layer region $0 < \eta < 4$ and it becomes minimum in the region $\eta > 4$ for all the values of ϵ. Figure 6(b) exhibits that with the increase in the value of ϵ, temperature of the fluid decreases in the boundary layer region $0 < \eta < 4$ and it becomes minimum in the region $\eta > 4$ for all the values of ϵ.Figure 6(c) exhibits that with the increase in the value of ϵ, concentration of the fluid increases in the boundary layer region $0 < \eta < 3.6$ and no effect is observed from $\eta = 3.6$ onwards.

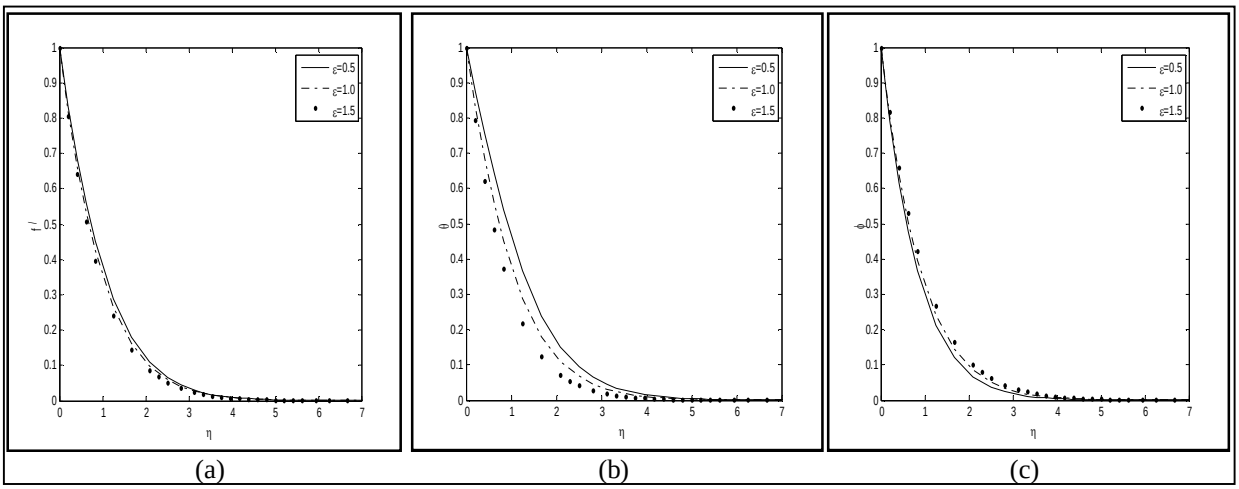

Figure 6 : Effect of pressure work parameter ϵ on (a) the velocity profiles, (b) the temperature profiles, (c) the concentration profiles

3.6. Case VI:

Figures 7(a)-(c) exhibits velocity, temperature and concentration profile for various values of heat source parameter Q. It is observed that the velocity, temperature and concentration decrease exponentially from their maximum values at the surface to their minimum values at the end of the boundary layer. Figure 7(a) exhibits that with the increase in the values of parameter Q, velocity of the fluid increases in the boundary layer region $0 < \eta < 4.2$ and it becomes minimum in the region $\eta > 4.2$ for all the values of Q. Figure 7(b) exhibits that with the increase in the value of Q, temperature of the fluid increases in the boundary layer region $0 < \eta < 4.8$ and no effect is observed from $\eta = 4.8$ onwards. Figure 7(c) exhibits that with the increase in the value of Q, concentration of the fluid decreases in the boundary layer region $0 < \eta < 4.2$ and no effect is observed from $\eta = 4.2$ onwards.

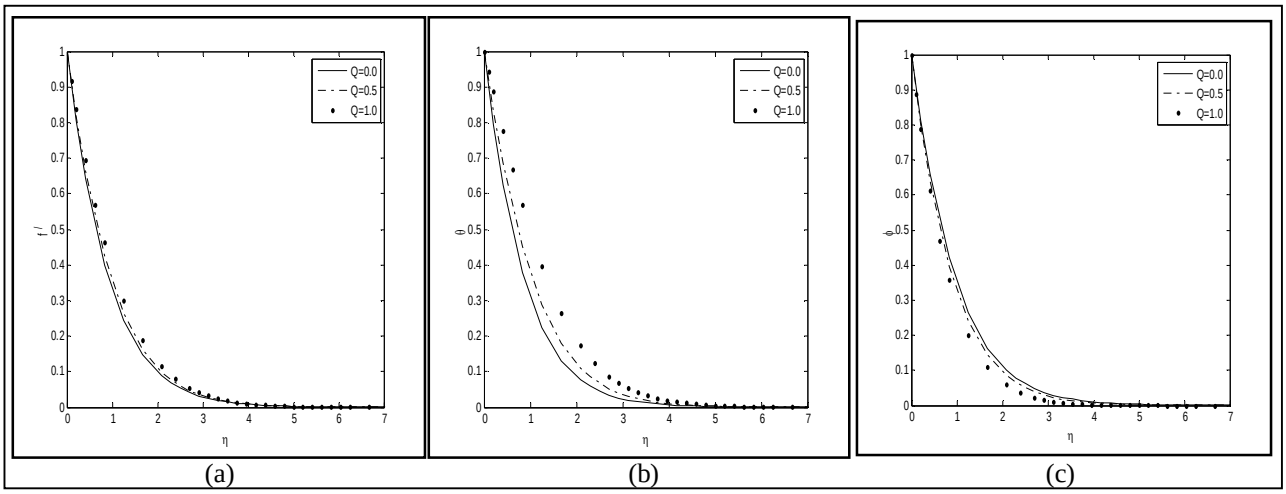

Figure 7: Effect of heat source parameter Q on (a) the velocity profiles, (b) the temperature profiles, (c) the concentration profiles

3.7. Case VII:

Figures 8(a)-(c) exhibits temperature and concentration profile for various values of Dufour number D_f It is observed that the velocity, temperature and concentration decrease exponentially from their maximum values at the surface to their minimum values at the end of the boundary layer. Figure 8(a) exhibits that with the increase in the values of parameter D_f, velocity of the fluid increases in the boundary layer region $0 < \eta < 2$ and reverse effect is noticed in the boundary layer region $2 < \eta < 4.2$. The velocity of the fluid becomes minimum in the region $\eta > 4.2$ for all the values of D_f Figure 8(b) exhibits that with the increase in the value of D_f, temperature of the fluid increases in the boundary layer region $0 < \eta < 3.2$ and reverse effect is observed $3.2 < \eta < 4.4$. The temperature of the fluid becomes minimum in the region $\eta > 4.4$ for all the values of D_f. Figure 8(c) exhibits that with the increase in the value of D_f, concentration of the fluid decreases in the boundary layer region $0 < \eta < 4.2$ and no effect is observed from $\eta = 4.2$ onwards.

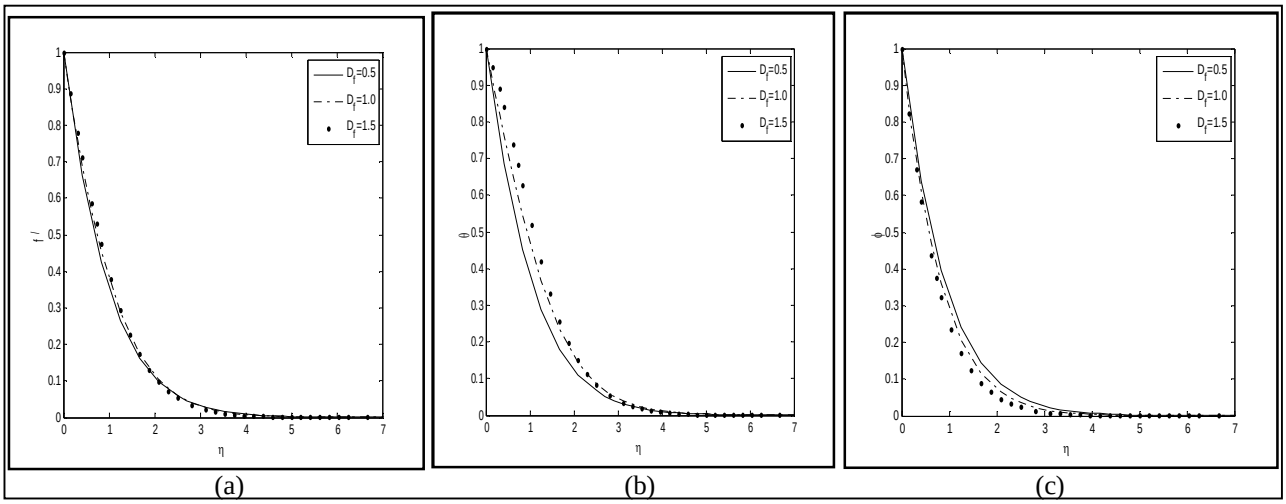

Figure 8: Effect of Dufour number D_f on (a) the velocity profiles, (b) the temperature profiles, (c) the concentration profiles

3.8. Case VIII:

Figures 9(a)-(c) exhibits velocity, temperature and concentration profile for various values of thermal stratification parameter n . It is observed that the velocity, temperature and concentration decrease exponentially from their maximum values at the surface to their minimum values at the end of the boundary layer. Figure 9((a)-(c)) exhibits that with the increase in the values of parameter n, velocity and temperature decreases slightly in the boundary layer region $0 < \eta < 4.4$ but concentration of the fluid increases slightly in the boundary layer region $0 < \eta < 4.4$ and no effect is observed from $\eta = 4.4$ onwards.The velocity , temperature and concentration of the fluid becomes minimum in the region $\eta > 4.4$ for all the values of n.

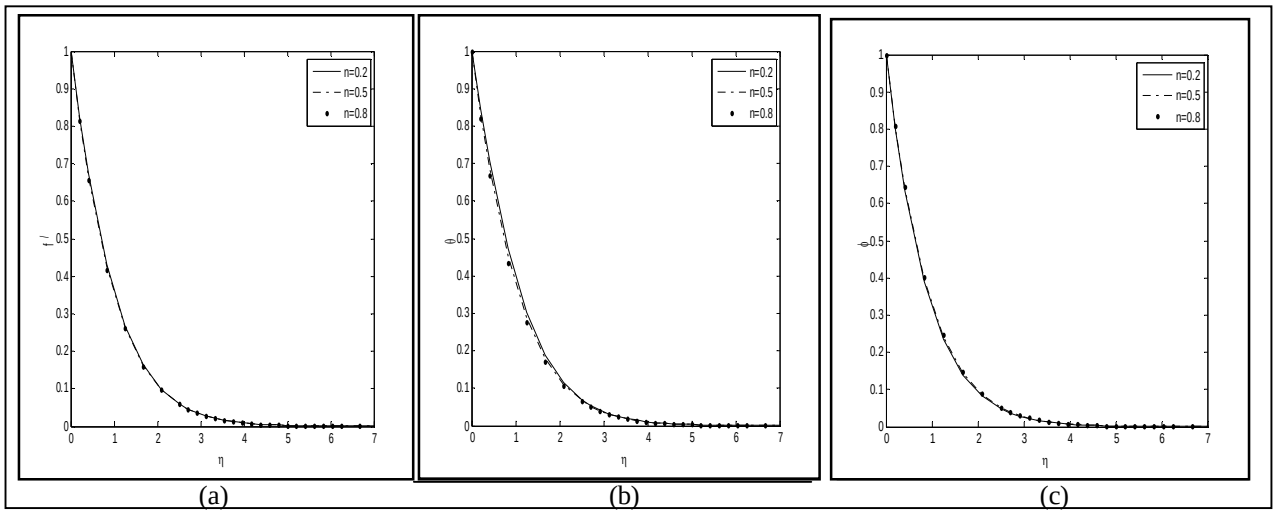

Figure 9: Effect of thermal stratification parameter n on (a) the velocity profiles, (b) the temperature profiles, (c) the concentration profiles

3.9. Case IX:

Figures 10(a)-(c) exhibits velocity, temperature and concentration profile for various values of Schmidt number Sc . It is observed that the velocity, temperature and concentration decrease exponentially from their maximum values at the surface to their minimum values at the end of the boundary layer. Figure 10(a) exhibits that with the increase in the values of parameter Sc, velocity of the fluid decreases in the boundary layer region $0 < \eta < 5$ and no effect is observed from η=5 onwards. Figure 10(b) exhibits that with the increase in the value of Sc, temperature of the fluid increases in the boundary layer region $0 < \eta < 4$ and no effect is observed from $\eta = 4$ onwards. Figure 10(c) exhibits that with the increase in the value of Sc, concentration of the fluid decreases throughout in the boundary layer region $0 < \eta < 7$.

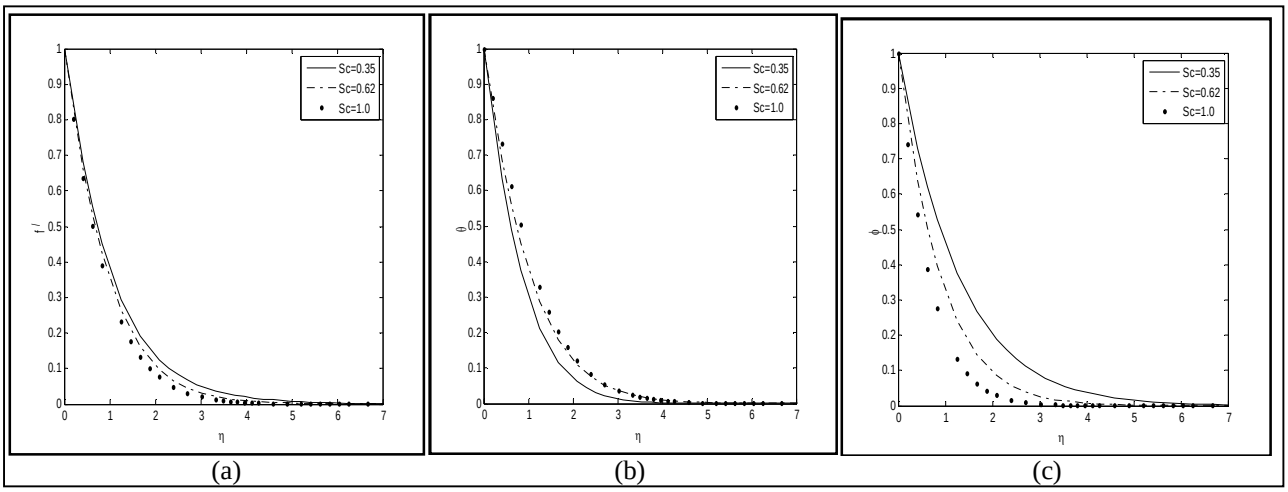

Figure 10: Effect of Schmidt number n on (a) the velocity profiles, (b) the temperature profiles, (c) the concentration profiles

3.10. Case X:

Figures 11(a)-(c) exhibits velocity, temperature and concentration profile for various values of chemical reaction parameter γ. It is observed that the velocity, temperature and concentration decrease exponentially from their maximum values at the surface to their minimum values at the end of the boundary layer. Figure 11(a) exhibits that with the increase in the values of parameter γ, velocity of the fluid decreases in the boundary layer region $0 < \eta < 4.4$ and no effect is observed from η= 4.4 onwards. Figure 11(b) exhibits that with the increase in the value of γ, temperature of the fluid increases in the boundary layer region $0 < \eta < 4.4$ and no effect is observed from $\eta = 4.4$ onwards. Figure 11(c) exhibits that with the increase in the value of γ, concentration of the fluid decreases throughout in the boundary layer region $0 < \eta < 4.2$ and no effect is observed from $\eta = 4.2$ onwards.

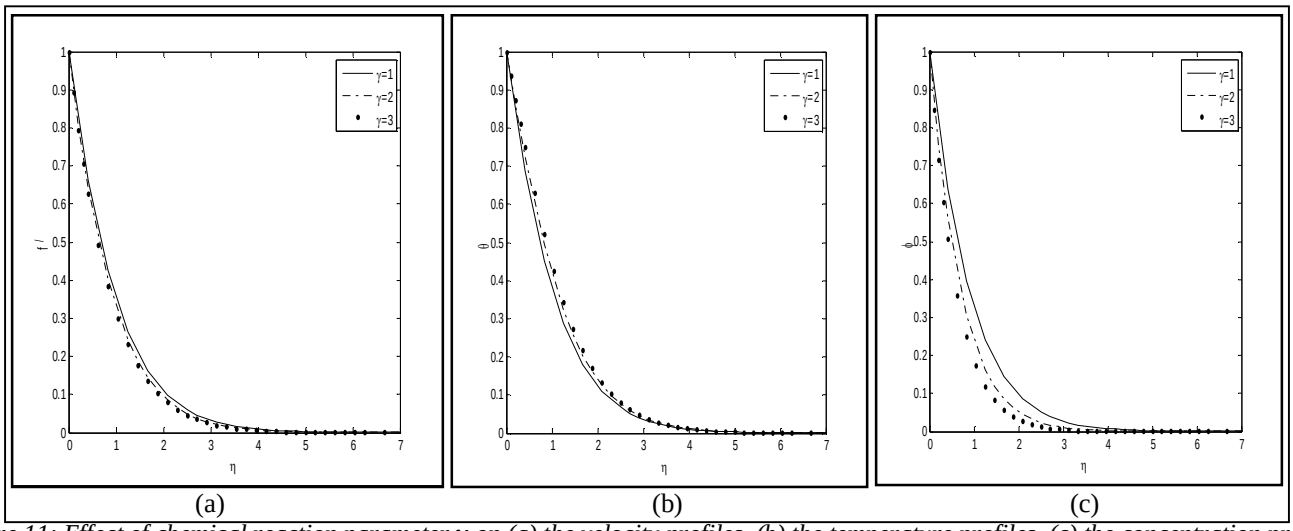

Figure 11: Effect of chemical reaction parameter γ on (a) the velocity profiles, (b) the temperature profiles, (c) the concentration profiles

3.11. Case XI:

Figures 12(a)-(c) exhibits temperature and concentration profile for various values of Soret number S_r . It is observed that the velocity, temperature and concentration decrease exponentially from their maximum values at the surface to their minimum values at the end of the boundary layer. Figure 12(a) exhibits that with the increase in the values of parameter S_r , velocity of the fluid increases in the boundary layer region $0 < \eta < 7$. Figure 12(b) exhibits that with the increase in the value of S_r, temperature of the fluid decreases in the boundary layer region $0 < \eta < 3$ but reverse effect is observed from $3 < \eta < 7$. Figure 12(c) exhibits that with the increase in the value of S_r , concentration of the fluid increases throughout in the boundary layer region $0 < \eta < 7$.

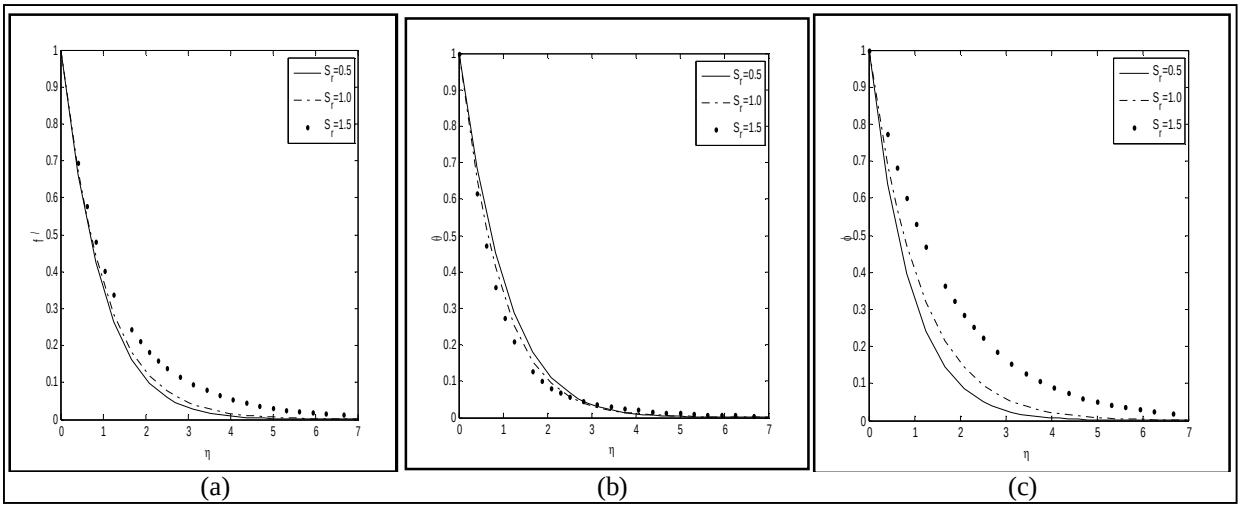

Figure 12: Effect of Soret number S_r on (a) the velocity profiles, (b) the temperature profiles, (c) the concentration profiles

3.12. Case XII:

Figures 13(a)-(c) exhibits temperature and concentration profile for various values of wall concentration exponent n_1 . It is observed that the velocity, temperature and concentration decrease exponentially from their maximum values at the surface to their minimum values at the end of the boundary layer. Figure 13(a) exhibits that with the increase in the values of parameter n_1 , velocity of the fluid decreases slightly in the boundary layer region $0 < \eta < 4.4$ and no effect is observed from $\eta = 4.4$ onwards.. Figure 13(b) exhibits that with the increase in the value of n_1, temperature of the fluid increases slightly in the boundary layer region $0 < \eta < 4.4$ and no effect is observed from $\eta = 4.4$ onwards. Figure 13(c) exhibits that with the increase in the value of n_1, concentration of the fluid decreases in the boundary layer region $0 < \eta < 4.6$ and no effect is observed from $\eta = 4.6$ onwards.

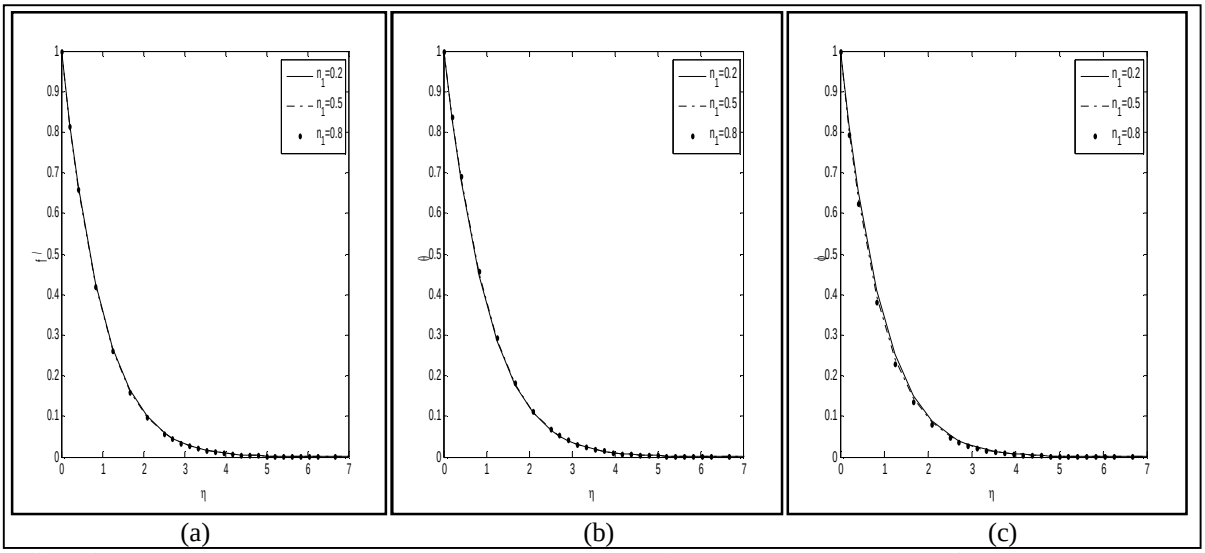

(a) (b) (c)

Figure 13: Effect of wall concentration exponent n_1 on (a) the velocity profiles, (b) the temperature profiles, (c) the concentration profiles

M	Ra	N	Pr	ε	Q	D_f	n	Sc	γ	S_r	n_1	$-\theta'(0)$	$-\emptyset'(0)$
1	1	1	0.71	1	0.5	0.5	0.5	0.62	1	0.5	0.5	0.8461	1.0257
2	1	1	0.71	1	0.5	0.5	0.5	0.62	1	0.5	0.5	0.5171	1.0021
3	1	1	0.71	1	0.5	0.5	0.5	0.62	1	0.5	0.5	0.2882	0.9958
1	0.5	1	0.71	1	0.5	0.5	0.5	0.62	1	0.5	0.5	0.2882	0.9958
1	1.0	1	0.71	1	0.5	0.5	0.5	0.62	1	0.5	0.5	0.8461	1.0258
1	1.5	1	0.71	1	0.5	0.5	0.5	0.62	1	0.5	0.5	1.2077	1.0692
1	1	0.5	0.71	1	0.5	0.5	0.5	0.62	1	0.5	0.5	0.6377	1.0060
1	1	1.0	0.71	1	0.5	0.5	0.5	0.62	1	0.5	0.5	0.8461	1.0257
1	1	1.5	0.71	1	0.5	0.5	0.5	0.62	1	0.5	0.5	1.0408	1.0468
1	1	1	0.71	1	0.5	0.5	0.5	0.62	1	0.5	0.5	0.8461	1.0257
1	1	1	1.0	1	0.5	0.5	0.5	0.62	1	0.5	0.5	1.0651	0.9579
1	1	1	2.0	1	0.5	0.5	0.5	0.62	1	0.5	0.5	1.8185	0.6703
1	1	1	0.71	0.5	0.5	0.5	0.5	0.62	1	0.5	0.5	0.5984	1.1029
1	1	1	0.71	1.0	0.5	0.5	0.5	0.62	1	0.5	0.5	0.8461	1.0258
1	1	1	0.71	1.5	0.5	0.5	0.5	0.62	1	0.5	0.5	1.0781	0.9540
1	1	1	0.71	1	0	0.5	0.5	0.62	1	0.5	0.5	1.0689	0.9566
1	1	1	0.71	1	0.5	0.5	0.5	0.62	1	0.5	0.5	0.8461	1.0257
1	1	1	0.71	1	1.0	0.5	0.5	0.62	1	0.5	0.5	0.5498	1.1171
1	1	1	0.71	1	0.5	0.5	0.5	0.62	1	0.5	0.5	0.8461	1.0257
1	1	1	0.71	1	0.5	1.0	0.5	0.62	1	0.5	0.5	0.5818	1.1107
1	1	1	0.71	1	0.5	1.5	0.5	0.62	1	0.5	0.5	0.2833	1.2136
1	1	1	0.71	1	0.5	0.5	0.2	0.62	1	0.5	0.5	0.7551	1.0528
1	1	1	0.71	1	0.5	0.5	0.5	0.62	1	0.5	0.5	0.8461	1.0257
1	1	1	0.71	1	0.5	0.5	0.8	0.62	1	0.5	0.5	0.9323	0.9989
1	1	1	0.71	1	0.5	0.5	0.5	0.35	1	0.5	0.5	1.0094	0.7327
1	1	1	0.71	1	0.5	0.5	0.5	0.62	1	0.5	0.5	0.8461	1.0257
1	1	1	0.71	1	0.5	0.5	0.5	1.0	1	0.5	0.5	0.6868	1.3786
1	1	1	0.71	1	0.5	0.5	0.5	0.62	1	0.5	0.5	0.8461	1.0257
1	1	1	0.71	1	0.5	0.5	0.5	0.62	2	0.5	0.5	0.7076	1.3304
1	1	1	0.71	1	0.5	0.5	0.5	0.62	3	0.5	0.5	0.6027	1.5745
1	1	1	0.71	1	0.5	0.5	0.5	0.62	1	0.5	0.5	0.8461	1.0257
1	1	1	0.71	1	0.5	0.5	0.5	0.62	1	1.0	0.5	0.9333	0.8619
1	1	1	0.71	1	0.5	0.5	0.5	0.62	1	1.5	0.5	1.0601	0.6167
1	1	1	0.71	1	0.5	0.5	0.5	0.62	1	0.5	0.2	0.8755	0.9551
1	1	1	0.71	1	0.5	0.5	0.5	0.62	1	0.5	0.5	0.8461	1.0257
1	1	1	0.71	1	0.5	0.5	0.5	0.62	1	0.5	0.8	0.8180	1.0935

TABLE 1: The values of rate of heat and mass transfer in terms of local Nusselt number $-\theta'(0)$ and local Sherwood number $-\emptyset'(0)$ for selected values of $M, Ra, N, Pr, \varepsilon, Q, D_f, n, Sc, \gamma, S_r$ and n_1.

4. Conclusions

In this work, chemical reaction, heat source, pressure work, thermal-diffusion and diffusion-thermal effects on MHD heat and mass transfer free convection flow over a stretching cone embedded in a porous medium has been investigated. From our investigation as obvious from table 1, we can conclude that the rate of heat transfer decreases in magnitude with increase in magnetic field, heat source, Dufour number, Schmidt number, chemical reaction parameter and wall concentration exponent but increases in magnitude with increase in Rayleigh number, buoyancy ratio parameter, Prandtl number, pressure work parameter, thermal stratification parameter and Soret number. We can also conclude from table 1 that the rate of mass transfer decreases in magnitude with increase in magnetic field, Prandtl number, pressure work parameter, thermal stratification parameter and Soret number, but increases in magnitude with increase in Rayleigh number, buoyancy ratio parameter, heat source, Dufour number, Schmidt number, chemical reaction parameter and wall concentration exponent.

5. References

i. Andersson, H. I., Hansen, O. R., & Holmedal, B. (1994). Diffusion of a chemically reactive species from a stretching sheet. Int. J. Heat Mass Transfer, 37, 659-664.

ii. Anjali Devi, S.P.,& Kandasamy, R. (1999). Effects of chemical reaction heat and mass transferon laminar flow along a semi infinite horizontal plate. Heat Mass Transfer, 35, 465-467.

iii. Muthucumarswamy, R.,& Ganesan, P. (2002). Effects of suction on heat and mass transferalong a moving vertical surface in the presence of chemical reaction. Forschung im Ingenieurwesen, 67, 129-132.

iv. Hering, R.G. (1965). Laminar free convection from a non-isothermal cone at low Prandtl numbers. Int. J. Heat Mass Transfer, 8, 1333-1337.

v. Roy, S. (1974). Free convection from a vertical cone at high Prandtl numbers. Transactions of ASME Journal of Heat Transfer, 96, 115-117.

vi. Yih, K.A. (1997). The effect of uniform lateral mass flux on free convection about a vertical cone embedded in porous media. Int. Commun. Heat Mass Transfer, 24, 1195-1205.

vii. Hossain, M.A., Vafai, K.,& Khanafer, K. (1999). Non-Darcy natural convection heat and mass transfer along a vertical permeable cylinder embedded in a porous medium. Int. J.Thermal Sci., 38, 854-862.

viii. Chamkha, A.J., Khaled, A.R.A.,& Al-Hawaj, O. (2000). Simultaneous heat and mass transfer by natural convection from a cone and a wedge in porous media. J. Porous Media, 3, 155-164.

ix. Mahdy, A., Mohamed, R.A., & Hady, F.M. (2008) . Influence of magnetic field on natural convection flow near a wavy cone in porous media. Latin American applied research, 38(2) , 155-160.

x. Muthucumaraswamy, R. (2002). The effects of a chemical reaction on a moving isothermal vertical infinitely long surface with suction. Acta Mechanica, 155, 65-70.

xi. Anjali Devi, S.P.,& Kandasamy, R. (2002). Effects of chemical reaction, heat and mass transfer on non-linear MHD laminar boundary layer flow over a wedge with suction and injection. Int. Commun. Heat Mass Transfer, 29, 707-716.

xii. Joshi, Y.,& Gebhart, B. (1981) Effect of pressure stress work and viscous dissipation in some natural convection flows. Int. J. Heat Mass Transfer, 24, 1577-1588.

xiii. Chamkha, A.J., & Mansour, M.A. (2012). Effects of chemical reaction and pressure work on free convection over a stretching cone embedded in a porous medium. Int.J. Industrial Mathematics, 4, 319-333.

xiv. Postelnicu, A. (2007). Influence of chemical reaction on heat and mass transfer by natural convection from vertical surfaces in porous media considering Soret and Dufour effects. Heat Mass Transf, 43, 595-602.[15] Cheng, C.Y. (2009). Soret and Dufour effects on natural convection heat and mass transfer from a vertical cone in porous media. Int. Commun. Heat and Mass Transfer, 36, 1020-1024. [16] Awad, F.G., Sibanda, P., Motsa, S.S.,& Makinde, O.D. (2011). Convection from an inverted cone in a porous medium with cross-diffusion effects. Computers and Mathematics with Applications, 61, 1431-1441.

xv. Chamkha. A.J.,& Rashad, A. (2014). Heat and Mass transfer by natural convection flow about a truncated cone in porous media with Soret and Dufour effects. Int.J. of Numerical Methods for heat and fluid flow , 24(3), 595-612.